NANOCRYSTALLINE N-TYPE SILICON FRONT SURFACE FIELD LAYERS: FROM RESEARCH TO INDUSTRY APPLICATIONS IN SILICON HETEROJUNCTION SOLAR CELLS

A.B. Morales-Vilches[1*], D. Decker[2], L. Mazzarella[1], L.Korte[1], R. Schlatmann[1],
D. Sontag[2], B. Stannowski[1]
[1]Helmholtz-Zentrum Berlin für Materialien und Energie GmbH, 12489 Berlin, Germany.
[2]Meyer Burger Germany, An der Baumschule 6-8, 09337 Hohenstein-Ernstthal, Germany

ABSTRACT: Nanocrystalline silicon and silicon oxide (nc-Si(O_x):H) layers grown by plasma-enhanced chemical vapor deposition (PECVD) have shown low parasitic absorption and excellent contact properties when implemented as n-type front surface field (FSF) contact in rear-junction silicon heterojunction (SHJ) solar cells [1-3]. In this contribution we present results from the successful process transfer from the lab at PVcomB at the Helmholtz-Zentrum Berlin (HZB), to the industrial pilot line at Meyer Burger Germany GmbH (MBG). Conversion efficiencies η > 22.5 % were demonstrated on SHJ cell (4 cm²) [2, 3]. The excellent cell performance in the lab and the potential to reduce parasitic absorption in the front stack by using nc-SiO_x:H motivated the process transfer from HZB to MBG. Initial cross processing experiments on 244 cm² wafers showed the benefit of using nc-Si:H as FSF layer. We here also emphasize the role of the Si texture on a fast nc-Si:H nucleation. After cross processing experiments a successful transfer of the nc-Si:H process and fine tuning resulted in a median cell efficiency of 23.4 %. This is in the same range as the MGB reference on 244 cm² cells, noteworthy, at the same throughput. Currently work is ongoing to further improve the optical performance of the cells by adding oxygen (CO_2).
Keywords: passivating contacts, transparent layers, silicon heterojunction solar cells.

1 INTRODUCTION

Silicon heterojunction (SHJ) solar cells have shown their efficiency potential and industrial relevance in the past years with world record efficiencies reported in all-back-contacted (26.7 % [4, 5]) and in 2-side contacted cells (24.5 % - 25.1 % [6, 7]). In these SHJ cells the p-type contact (junction) is usually placed at the front side. Placing it on the rear side instead allows to use n-doped nc-Si(O_x):H as the n-type contact, which exhibits excellent transparency and reaches a higher conductivity than its p-type counterpart. In recent papers we presented this, analyzing the optical benefit of (very thin) nc-SiO_x:H layers used on the cell's front side [1 - 3]. Now we incorporate our best processes in full-area cells in an industrial line in collaboration with MBG. In addition, the benefit of using these layers was shown in solar cells cross-processed at HZB and MBG, where most PECVD films were deposited at HZB and back-end processes done at MBG.

2 MATERIALS AND METHODS

Two different cell layouts were used to fabricate the rear junction silicon heterojunction solar cells (SHJ). Schematics of the device structure and pictures of the layouts are shown in fig. 1. A first layout of 14 small area (4 cm²) devices per wafer was used for the lab scale samples done at HZB. Detailed information about the different fabrication steps were shown elsewhere [2]. A second layout of full area cells (244.3 cm²) was used for the fab scale samples done both at HZB and at MBG. In this study we focus on the development of the front n-type silicon layers deposited by plasma enhanced chemical vapor deposition (PECVD).

2.1 Lab scale SHJ solar cells

Initially lab scale samples were used to analyze the different materials used as n-doped front contact (FSF) deposited by PECVD in an Applied Materials AKT1600 cluster tool for max. four wafers per run. Amorphous and nanocrystalline n-type layers have been already compared in a previous paper [2] demonstrating the benefit both optically and electrically when using the nanocrystalline material as FSF. The optical benefit of introducing oxygen in these layers has also been studied in the past in our group [1-3]. In this work we aimed to transfer the processes for these PECVD deposited layers to the industrial like HELiA PECVD tool from MBG with the capability of processing 6 inch wafers (56 wafers per run) at high throughput (>2400 wafers per hour).

2.2 Fab scale SHJ solar cells

The full-area SHJ solar cells were manufactured both at the lab at HZB and at the industrial like pilot line at MBG. In order to transfer the technology from "lab" to the "fab", cross-experiments between the two sites were done first to show the potential of these materials: front end processes at HZB (wet chemistry and PECVD) and back end processes at MBG (PVD for TCO and metal screen printing). The process transfer was then done first for the non-oxidic nc-Si layer. Once this layer was successfully implemented, oxygen (CO_2) was added to further optically improve the material.
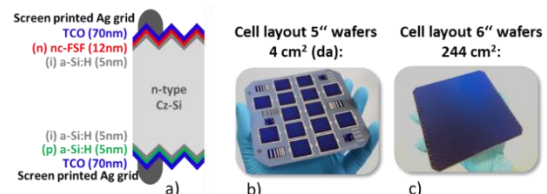

Figure 1: a) Cross section view of the bifacial rear-emitter silicon heterojunction (SHJ) solar cell studied in this work with ITO as the TCO and nanocrystalline Si front surface field layers; b) Cell layout of 4 cm² busbar-less cells on Cz-Si wafers and c) full-area busbar-less cells with a total area of 244.3 cm².

3 RESULTS AND DISCUSSION

Table 1 presents SHJ cell parameters obtained at HZB directly comparing nc-Si:H and nc-SiO$_x$:H FSF with efficiencies of 22.3% and 22.8 %, respectively. A net J$_{sc}$ gain of +0.6 mA/cm² is found for cells with the oxidic layer. Full area cells (244 cm²) with nc-SiO$_x$:H FSF were then processed at HZB reaching 21.4 % [3]. Despite a comparable J$_{sc}$ measured we could not yet reproduce the same efficiency level as obtained on small cells since the back-end processes for full size cells were not fully optimized. Therefore, in parallel we started cross processing experiments together with MBG, thereby, benefiting from the established full-size cell processes at MBG.

Table I: Nanocrystalline silicon (oxide) layer properties refractive index n at 632 nm wavelength and lateral conductivity σ, as derived from thick layers grown on glass and SHJ cell parameters using these layers as FSF. The J$_{sc}$ results clearly show the optical benefit of the oxidic FSF due to lower parasitic absorption. Since the other electrical parameters keep the same excellent level, the optical benefit is transferred directly into the final conversion efficiency.

| nc-	Single layers on glass		Cell results (4 cm²)			
	n	σ [S/cm]	J$_{sc}$ [mA/cm²]	V$_{oc}$ [mV]	FF [%]	η [%]
Si:H	3.7	62	38.3	727	80.0	22.3
SiO$_x$:H	2.7	0.8	38.9	730	80.1	22.8

To demonstrate the potential of the nc-Si(O$_x$):H layers developed at HZB the back-end processes for full area cells were done at MBG. Fig. 2 shows results of co-deposited cells on different wafer textures. Sample 1 with a larger pyramid size and a clear roughness on the pyramid facets reveals a detrimental effect in cell performance compared to Sample 2, which has a much smaller pyramid size and appears to have more smooth pyramid facets. These samples demonstrate that the surface topography has a critical influence on the cell performance when implementing nanocrystalline Si layers. We attribute this in particular to a certain degree of nano-roughness on the pyramid facets (compare Figs. 2b and 2c). This might disturb or delay the nc-Si:H nucleation resulting in lower crystalline fraction in very thin layers and, hence, increases parasitic absorption and lowers conductivity. As a result J$_{sc}$ as well as FF and V$_{oc}$ are reduced, the latter two due to an increased contact resistance and a reduced field-effect passivation.

After adapting the texturing process, a larger cross processing experiment with both nc-Si:H and nc-SiO$_x$:H FSF layers was carried out. Fig. 3 shows the results of four different experiments carried out between HZB and MBG, as described in the sketch in the lower part of the figure. The first three splits consist of 6 wafers each, while split 4 (dark blue) the reference devices with a-Si:H FSF, was fully processed at MBG and included about 100 wafers. Split 3 shows the same MBG reference but with the wet chemical processes performed at HZB. We ascribe the lower cell performance in this group to sample shipment between critical process steps, which probably led to Si surface deterioration in this split group. Therefore, in splits

1 and 2 both wet chemistry and PECVD were done at HZB within a very short time. In split 1 (orange) nc-Si:H was used as the FSF while the green group corresponds to the nc-SiO$_x$:H FSF samples. The high V$_{oc}$ and FF of the nc-Si:H samples leads to an increase in the median η by 0.15% (split 1) compared to the reference in split 4. The optical benefit of the split 2 with the oxidic FSF is clearly visible in the J$_{sc}$, however, the FF is not yet as good as in the non-oxidic samples. Currently, the focus is on optimizing the deposition parameters to improve the FF of the cells using the nc-SiO$_x$:H FSF layers in 6-inch full area devices in the line at MBG.
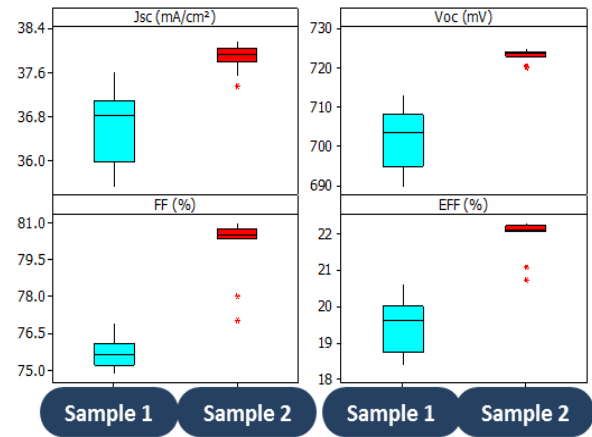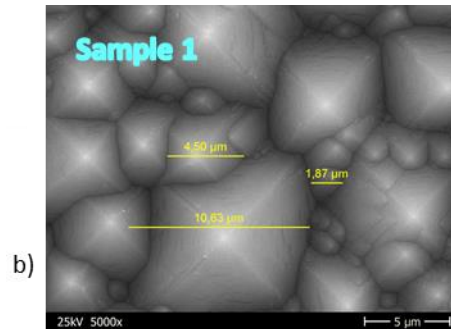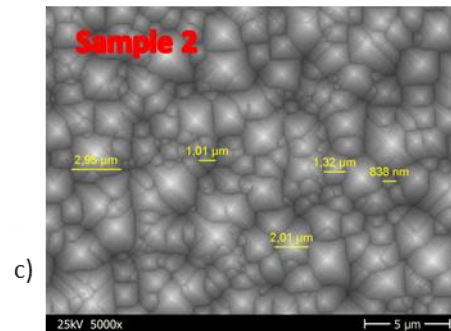
Figure 2: a) Solar cell characteristics of first cross-processed full-area size (244 cm²) SHJ solar cells using two texturing processes. The same nc-Si:H FSF was deposited at HZB in both samples to directly compare the texturing effect. Each boxplot includes the results of 6 wafers from the same sample group. b) and c) SEM images of the two differently textured wafers.
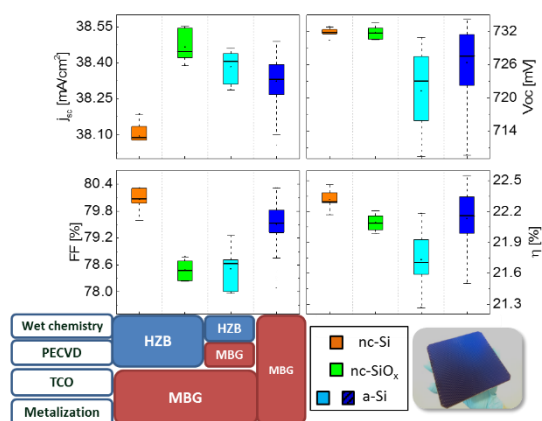
Figure 3: Solar cell characteristics of full area SHJ cells (244.3 cm²) from a cross processing experiment with four groups (split 1 – 4) carried out jointly by HZB and MBG on Cz-Si wafers with the optimized small-pyramid texture used for all groups (compare to sample 2 in Fig. 2c). In the lower left part a sketch of the different process splits clarifies where the different process steps were done. In the lower right part a picture of the full-area cell devices is shown.

After the cross experiments the challenge was to transfer the PECVD processes from the Applied Materials AKT1600 cluster system at HZB, to the industrial large-area and high-throughput Helia system at MBG (56 wafers per run). As a result the nc-Si:H process was successfully implemented obtaining efficiencies on the same level as the amorphous reference process at MBG, even maintaining the same throughput (fig. 4). The transfer for the oxidic layer (nc-SiOx:H) was also started, obtaining efficiencies in the 23% range independent of the nc-layer used. There is still some room for improvement in the oxidic layer due to the lower FF, which prevents from obtaining the full potential of this material, in terms of optical gain. Additionally, both transferred nc-layers had an excellent homogeneity in all the tray, as can be observed from the solar cell efficiency and electroluminescence images from all the samples on the complete tray depicted in figure 5. Here only solar cells that use the nc-Si:H without oxygen are shown but the homogeneity was equally reproduced in the oxidic nc-layer.
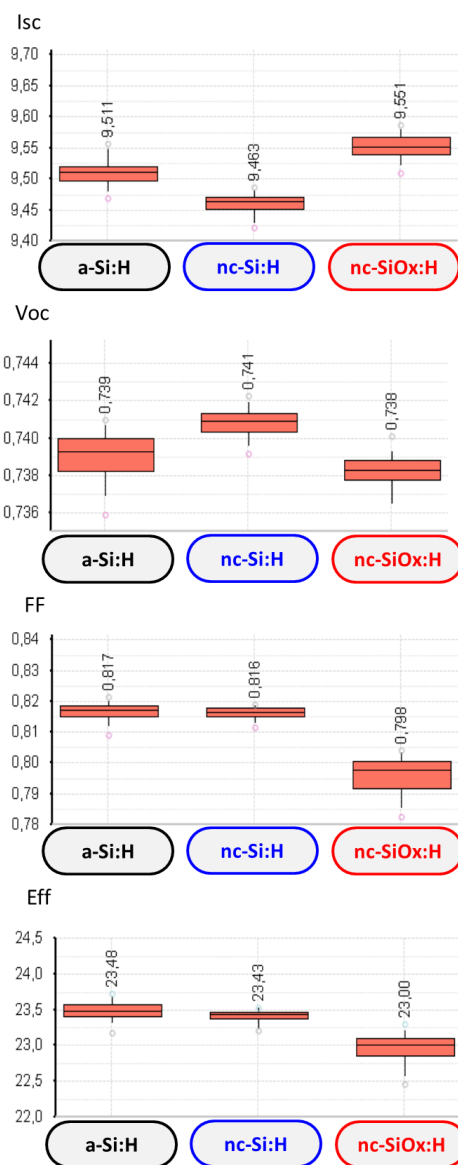

Figure 4: Solar cell characteristics of full area size SHJ cells (244.3 cm²) using three different n-type layers deposited at the MGB pilot line PECVD tool (Helia).
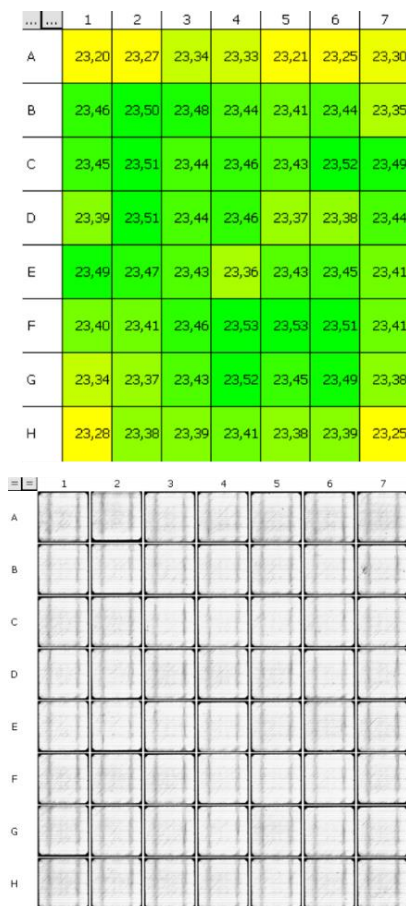
...	1	2	3	4	5	6	7
A	23,20	23,27	23,34	23,33	23,21	23,25	23,30
B	23,46	23,50	23,48	23,44	23,41	23,44	23,35
C	23,45	23,51	23,44	23,46	23,43	23,52	23,49
D	23,39	23,51	23,44	23,46	23,37	23,38	23,44
E	23,49	23,47	23,43	23,36	23,43	23,45	23,41
F	23,40	23,41	23,46	23,53	23,53	23,51	23,41
G	23,34	23,37	23,43	23,52	23,45	23,49	23,38
H	23,28	23,38	23,39	23,41	23,38	23,39	23,25

Figure 5: Solar cell efficiency and electroluminescence images of all the wafers deposited in the same PECVD tray. In that case using the nc-Si:H.

4. CONCLUSIONS

In this work we obtained excellent performance of full size (244.3 cm²) cells with nc-Si:H as the FSF layer and a clear optical benefit of the nc-SiO$_x$:H FSF with a J$_{sc}$ increase of +0.5 mA/cm². Different from the lab results, nc-SiO$_x$:H results in the cross experiment leads to a slight FF loss. The excellent results with the nc-Si:H FSF triggered the process transfer to the MBG pilot line which was done successfully, surpassing the cell efficiency of 23% for both nc-Si:H and nc-SiO$_x$:H n-type layers. We observed still a lower FF for the cells with the oxidic layer, which needs to be solved in future in order to benefit from the full potential of this material. Besides cell efficiency also the production requirements were fulfilled, such as high throughput (60s PECVD process time) and excellent cell homogeneity over the 56 wafers on the PECVD tray. Moreover, it was demonstrated in the MBG pilot line that the nc-Si:H PECVD process is very reproducible and stable over time.

REFERENCES

[1] L. Mazzarella et al., "Nanocrystalline n-type Silicon Oxide Front Contacts for SHJ solar cells: Photocurrent Enhancement on Planar and Textured Substrates",IEEE J-PV, Vol. 8 (2017), 70-78.

[2] A. Morales et al., "Nanocrystalline vs. amorphous n-type silicon front surface field layers in SHJ solar cells: Role of thickness and oxygen content", Proc. of EUPVSEC 2017, Amsterdam.

[3] L. Mazzarella et al., "Ultra-thin nanocrystalline n-type silion oxide front contact layers for rear-emitter silicon heterojuntion solar cells", 179, 386-391 Sol. En. Mat, 2018.

[4] K. Yoshikawa et al., "Exceeding conversion efficiency of 26% by heterojunction interdigitated back contact solar cell with thin film Si technology", Solar Energy Materials and Solar Cells 173, December 2017, Pages 37-42.

[5] M. A. Green et al., "Solar cell efficiency tables (version 50)", Prog. Photovolt. Res. Appl. 2017; 25:668–676. https://doi.org/10.1002/pip.2909.

[6] M. Tauchi et al., "24.7% Record Efficiency HIT Solar Cell on Thin Silicon Wafer", IEEE J-PV, 4 (2014) 96-99.

[7] D. Adachi et al., "Impact of carrier recombination on fill factor for large area heterojunction crystalline silicon solar cell with 25.1% efficiency", Applied Physics Letters 107, 233506 (2015); doi: 10.1063/1.4937224.